Templated-PISA: Driving Polymerization-Induced Self-Assembly towards the Fibre Morphology

Gaëlle Mellot, Jean-Michel Guigner, Laurent Bouteiller, François Stoffelbach, Jutta Rieger

To cite this version:

Gaëlle Mellot, Jean-Michel Guigner, Laurent Bouteiller, François Stoffelbach, Jutta Rieger. Templated-PISA: Driving Polymerization-Induced Self-Assembly towards the Fibre Morphology. Angewandte Chemie, 2019, 131 (10), pp.3205-3209. 10.1002/anie.201809370 . hal-02353709

HAL Id: hal-02353709
https://hal.sorbonne-universite.fr/hal-02353709v1

Submitted on 7 Nov 2019

Templated-PISA: Driving Polymerization-Induced Self-Assembly towards the Fibre Morphology

Gaëlle Mellot,[a] Jean-Michel Guigner,[b] Laurent Bouteiller,[a] François Stoffelbach*[a], and Jutta Rieger*[a]

Abstract: *Dispersions of block-copolymer fibres in water have many potential applications and can be obtained by polymerization-induced self-assembly (PISA), but only in very restricted experimental conditions. In order to enlarge this experimental window, we introduced a supramolecular moiety, a hydrogen-bonded bis-urea sticker, in the macromolecular reversible addition-fragmentation chain transfer agent to drive the morphology of the nano-objects produced by RAFT-mediated PISA towards the fibre morphology. This novel concept is tested in the synthesis of a series of poly(N,N-dimethylacrylamide)-b-poly(2-methoxyethyl acrylate) (PDMAc-b-PMEA) diblock copolymers prepared by dispersion polymerization in water. The results prove that the introduction of the templating bis-urea stickers into PISA greatly promotes the formation of fibres in a large experimental window.*

Thanks to the development of polymerization-induced self-assembly (PISA), it is nowadays possible to produce amphiphilic block copolymer assemblies in a straightforward way, in high yield and at high solids contents (typically 10-40 wt%), through green, water-based processes.[1-5] Among the PISA techniques operative in water the most popular and versatile one is to perform a reversible addition fragmentation chain transfer (RAFT)[6] radical polymerization of a monomer with limited water-solubility from a hydrophilic macromolecular chain transfer (macro-RAFT) agent. Beyond a certain degree of polymerization, the formed block becomes insoluble in the polymerization medium and amphiphilic block copolymers are synthesized that self-assemble into particles. Their morphology, mainly spheres, worms/fibres or vesicles, is principally determined by the block lengths, which affect the packing parameter.[7-11] Fibres are a particularly interesting structure: thanks to their high aspect ratio, numerous applications can be considered in material science such as their use as hydrogels for biomedical application,[12] rheology modifiers,[13-15] pickering emulsifiers[16] or to reinforce water-borne coatings.[17] However, their development remains challenging, in particular because of the insufficient versatility of the existing synthetic methods. Indeed, for a selected diblock copolymer, the experimental window to reach the worm/fibre morphology is currently very narrow[2,18-20] so that laborious experimental fine tuning of the block lengths and of the solids content, at which the polymerizations are performed, is necessary. Importantly, as the particle morphology depends on the molar mass of the blocks, it is not possible to tune the fibre diameter at will. Moreover, sometimes only mixed phases are obtained. Finally, reproducibility issues make scale up production very difficult, and it is nowadays clearly recognized that new strategies towards the reproducible production of well-defined anisotropic morphologies are highly desirable.[21] For instance, photo-PISA at room temperature is now a reliable mean to reach temporal control over the nanoparticle morphology and favour the formation of anisotropic morphologies.[22-24] In the case of block copolymer assemblies prepared post-polymerization by annealing strategies or co-solvent methods[25], it is possible to overrule the packing-parameter-dependent morphology control and to obtain mainly filamentous nanostructures by crystallization of the hydrophobic block.[26-29] The main advantage of crystallization-driven self-assembly is the possibility to control the fibre length *via* a seeded-growth strategy, however feasible only at very low polymer concentrations (generally far below 1 wt%). Another strategy is to introduce supramolecular structure-directing units in the polymer chains.[30,31] Note that, to the best of our knowledge, the synthesis of these supramolecularly engineered amphiphilic block-copolymers was only achieved in organic solvent and thereby the final assemblies were obtained in water by an indirect process and/or at low solids contents (typically 1 wt%). In this context, and inspired by hydrogen bonded fibrillar assemblies in water,[32-38] we propose a new concept: the introduction of a supramolecular sticker, a hydrogen bonded bis-urea, in the macro-RAFT agent structure in order to force PISA in water towards the fibre morphology, and thereby increase drastically the experimental window to reach this morphology. Thanks to this strategy, the preparation of anisotropic structures by PISA should become much more robust in terms of synthetic conditions and pave the way towards the design of new functional materials.

To prove the concept, poly(*N,N*-dimethylacrylamide) (PDMAc) and poly(2-methoxyethyl acrylate) (PMEA) were selected as the hydrophilic and hydrophobic blocks, respectively, and a novel bis-urea functionalized RAFT agent was designed (Scheme 1) to insert structure-directing stickers in the copolymers. The urea containing trithiocarbonate (TTC) macro-RAFT agent (**P1**, Table S1) was prepared by RAFT polymerization of DMAc in *N,N*-dimethylformamide (DMF) at 70 °C in the presence of TTC-U_2 (see SI) and 2,2′-azobis(isobutyronitrile) (AIBN) as an initiator. Size exclusion chromatography (SEC) analysis (Figure S6A) showed the formation of a polymer with low molar mass dispersity ($Đ$ = 1.17). The number-average molar mass (M_n) determined by ^{1}H NMR (M_n = 4.1 kg mol^{-1}) was consistent with the theoretical M_n. This macro-RAFT agent could be readily dissolved in water. Cryogenic transmission electron microscopy (cryo-TEM) analysis of a 1 wt% aqueous solution of **P1** showed a mixture of spheres and fibres (Figure S6B). By analogy with other urea-containing amphiphiles,[35-38] we propose that interactions between bis-urea moieties are responsible for the (at least partial) assembly into anisotropic objects. To confirm this, a blank (urea-free) macro-RAFT agent possessing an octadecyl chain was synthesized in similar conditions (Scheme 1, **P4** in Table S1, Figure S7A). Cryo-TEM images revealed the formation of spherical objects only (Figure S7B), confirming the critical role of the urea groups in the formation of the anisotropic morphology.

---

[a] G. Mellot, Dr. L. Bouteiller, Dr. F. Stoffelbach, Dr. J. Rieger
Sorbonne Université, CNRS
Institut Parisien de Chimie Moléculaire, UMR 8232, Equipe Chimie des Polymères
F-75252 Paris Cedex 05 (France)
E-mail: francois.stoffelbach@sorbonne-universite.fr and jutta.rieger@sorbonne-universite.fr

[b] Dr. J.-M. Guigner
Sorbonne Université, CNRS
Institut de Minéralogie, de Physique des Matériaux et de Cosmochimie, UMR 7590 - IRD - MNHN
F-75252 Paris Cedex 05 (France)

Supporting information and the ORCID identification number(s) for the author(s) of this article can be found under:
|https://doi.org/10.1002/anie.2018XXXXX

Scheme 1. (A) Structures of the RAFT agents TTC-U_2 and TTC-C_{18}. (B) Synthesis of PDMAc macro-RAFT agents and their chain extension yielding PDMAc$_x$-*b*-PMEA$_y$ diblock copolymers.

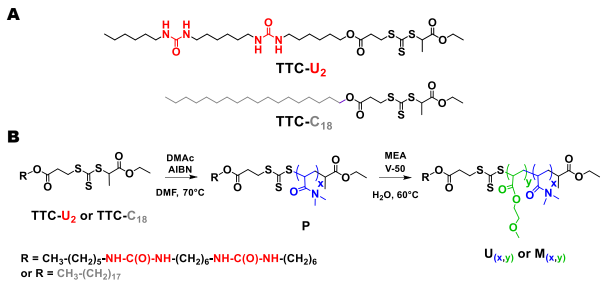

These macro-RAFT agents were then chain-extended by dispersion polymerization of MEA in water at 60 °C, using 2,2'-azobis(2-amidinopropane) dihydrochloride (V-50) as an initiator (**U1-U13, M1-M5**, Table S2). Polymerizations were performed at monomer contents varying from ~5 to ~29 wt%. In all cases, stable dispersions were obtained and high monomer conversions (> 80%) were generally reached within 4 h. SEC investigations showed independently of the macro-RAFT agent structure (with or without urea moieties) a complete shift of the macro-RAFT agent signal to high molar masses attesting the excellent blocking efficiency of the polymerizations. Furthermore, for all synthesized diblock copolymers low dispersities (below 1.4) were obtained. Monitoring a typical polymerization (**U8** in Table S2, Figure S8) showed that in the course of the polymerization the M_n increased linearly with monomer conversion and dispersities were low at all conversions ($Đ \leq 1.3$). All these results provide evidence for a good control over the MEA polymerization.

The morphology of the PDMAc$_x$-*b*-PMEA$_y$ diblock copolymer assemblies in water was investigated by cryo-TEM: PDMAc$_{35}$-*b*-PMEA$_{92}$-TTC-U_2 (**U6$_{(35,92)}$**) formed long nanofibres while the strict counterpart without urea PDMAc$_{33}$-*b*-PMEA$_{92}$-TTC-C_{18} (**M2$_{(33,92)}$**) formed only spherical objects (Figures 1A and 1B, Table S2). In conventional PISA, the particle morphology typically evolves (from spheres to worms/fibres to vesicles) when increasing the block length, *i.e.* molar mass of the hydrophobic block.[1-5] A series of block copolymers was therefore synthesized from a given macro-RAFT agent, at a fixed monomer concentration (~10 wt%) varying the length of the hydrophobic block. Whether the number-average degree of polymerization (DP_n) of PMEA was drastically reduced to 39 or increased to 151 (**U5-U7**, Table S2) only fibres were observed (Figures 1C and 1D). Moreover, by increasing the DP_n of PMEA the fibre diameter (D) increased from 13 ± 2 nm (DP_n = 39) to 17 ± 3 nm (DP_n = 92) and up to 25 ± 5 nm (DP_n = 151). For an even longer hydrophobic block length (DP_n = 224) (**U8**, Table S2), anisotropic nano-objects are still observed; nevertheless, at this stage steric hindrance effects of the growing hydrophobic block seem to counterbalance hydrogen-bonding interactions and thus significantly shorter fibres (with D = 28 ± 5 nm) were obtained (Figure S9).[39,40]

For conventional PISA, the morphology also depends on monomer concentration.[1-5] A too low monomer concentration may inhibit the formation of (pure) higher order morphologies (worms/fibres or vesicles), whereas a too high concentration may lead to colloidal stability issues. We therefore performed syntheses of PDMAc$_{35}$-*b*-PMEA$_{91}$-TTC-U_2 at various monomer concentrations (**U2**, **U4**, **U6**, **U9** and **U12**, Table S2). Cryo-TEM analyses of the resultant polymer dispersions (Figures 1A and 2) showed that long fibres were formed over a large monomer concentration range, from 7.3 wt% up to 28.0 wt% (Figures 1A, 2B, 2C and 2D). Only at the lowest concentration (~ 5 wt%) short fibres were mainly obtained (Figure 2A).

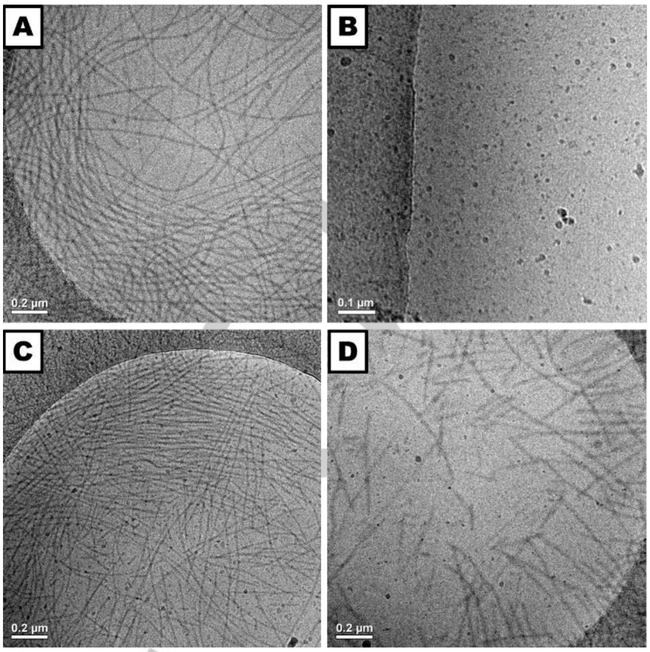

Figure 1. Cryo-TEM images of **U6$_{(35,92)}$** (A), **M2$_{(33,92)}$** (B), **U5$_{(34,39)}$** (C) and **U7$_{(34,151)}$** (D) prepared by templated-PISA at 10 wt% of monomer. The dark spots are contaminations stemming from water crystals on the sample surface.

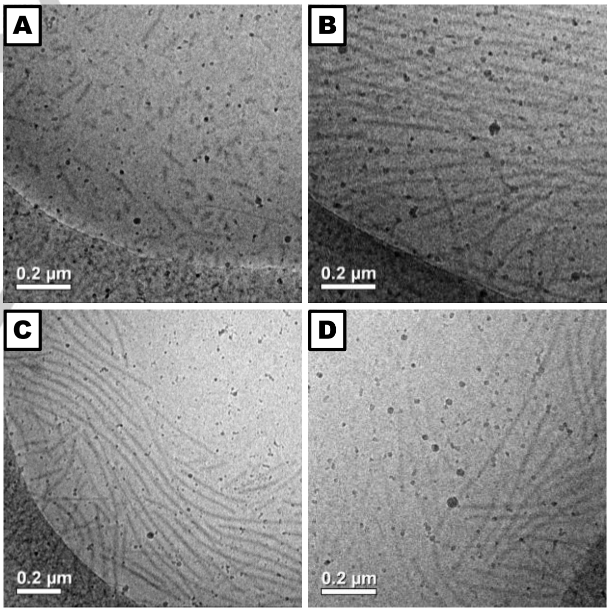

Figure 2. Cryo-TEM images of PDMAc$_{35}$-*b*-PMEA$_{91}$-TTC-U_2 diblock copolymers prepared at various monomer concentrations: 5.0 wt% **U2** (A), 7.3 wt% **U4** (B), 18.2 wt% **U9** (C) and 28.0 wt% **U12** (D). The dark spots are contaminations stemming from water crystals on the sample surface.

The pseudo phase diagram in Figure 3A summarizes all the results obtained by varying the hydrophobic block length and the monomer content (additional cryoTEM images are available in the SI, see Figure S10). It shows that the experimental window of the pure fibre phase is very large.

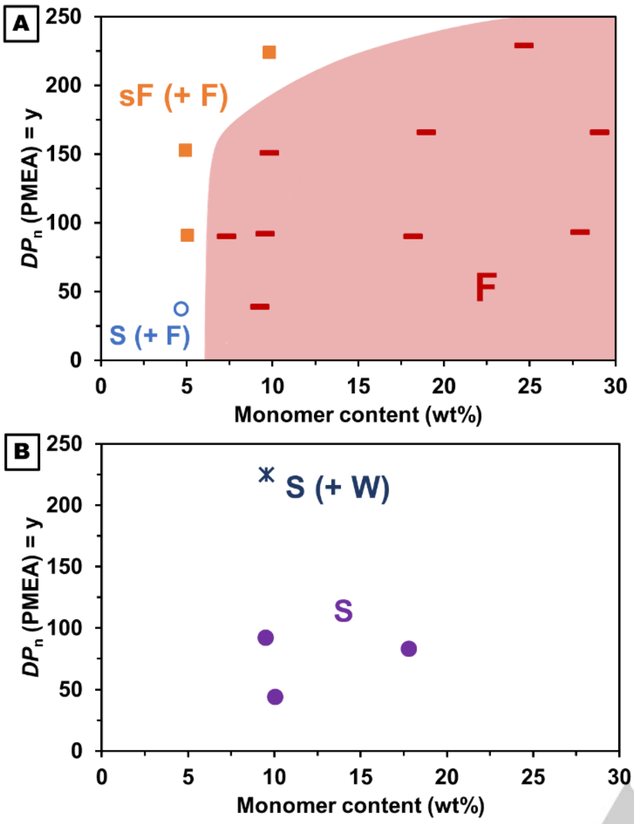

Figure 3. Pseudo phase diagrams for **PDMAc$_{35}$-*b*-PMEA$_y$-TTC-U$_2$** (A) and **PDMAc$_{33}$-*b*-PMEA$_y$-TTC-C$_{18}$** (B) diblock copolymers prepared at various monomer concentrations. The red domain represents the pure long-fibre phase. Dash = fibres (F), full circle = spheres (S), empty circle = mainly spheres with few fibres, square = mainly small fibres (sF) with few fibers, cross = mainly spheres with few worms (W).

To further prove the role of the urea sticker, we prepared a reference series of bis-urea-free copolymers (**M1**$_{(34,44)}$, **M2**$_{(33,92)}$, **M3**$_{(34,225)}$ and **M4**$_{(33,83)}$, Table S2), and the "model" pseudo phase diagram was established (Figure 3B). This diagram shows that block copolymers without urea stickers form mainly spherical objects (Figures 1B and S11), although they were prepared in the same polymerization conditions as their urea-containing counterparts, corroborating the crucial role of the bis-urea sticker in this templated-PISA mechanism.

The robustness of the system was further studied by varying the *DP*$_n$, *i.e.* the length, of the hydrophilic block. Macro-RAFT agents with *DP*$_n$ = 22 (**P2**, Table S1) and *DP*$_n$ = 11 (**P3**, Table S1) were synthesized in similar conditions as **P1** (*DP*$_n$ = 35). Owing to solubility issues, these macro-RAFT agents were chain-extended at lower temperature, either at 45 °C (**U14-U17**, Table S3) or 37 °C (**U18** and **U19**, Table S4) using 2,2'-azobis(*N,N*-dimethyleneisobutyramidine) dihydrochloride (VA-044) as an initiator. The morphologies of the resulting PDMAc$_x$-*b*-PMEA$_y$-TTC-U$_2$ copolymers assemblies, called **U**$_{(x,y)}$, prepared at 10 wt% were determined by cryo-TEM (Figures S12 and S13) and a phase diagram was constructed including the experimental results for various *DP*$_n$ of the hydrophilic (x) and the hydrophobic block (y) (Figure 4). Overall, the pseudo-phase diagram shows that the fibre morphology is obtained for a wide molar mass range. Examining the cryo-TEM images (Figures S12 and S13), it appears that the fibres obtained with the lower *DP*$_n$ macro-RAFT agents tend to be shorter than the former series. This effect is not elucidated at present, but might be related to the different polymerization conditions. For the lowest hydrophobic *DP*$_n$ (**U14**$_{(22,48)}$ and **U18**$_{(11,23)}$) a few spheres were also observed. Some aggregates were observed (by the naked eye) for sample **U15**$_{(11,97)}$, a highly asymmetric copolymer, obtained with the shortest macro-RAFT agent **P3**. In fact, some colloidal stability issues were observed for all PDMAc$_{11}$-*b*-PMEA$_y$-TTC-U$_2$ copolymers with y ≥ 100 (Figure 4). In view of the literature[41], this macroRAFT agent is certainly too short to stabilize efficiently the particles. It should be noted that reference experiments with the corresponding urea-free macroRAFT agents have also been performed, **M5a**$_{(19,60)}$ and **M5b**$_{(19,139)}$, and again, only spherical particles and no fibres were observed (Table S2, Figure S14).

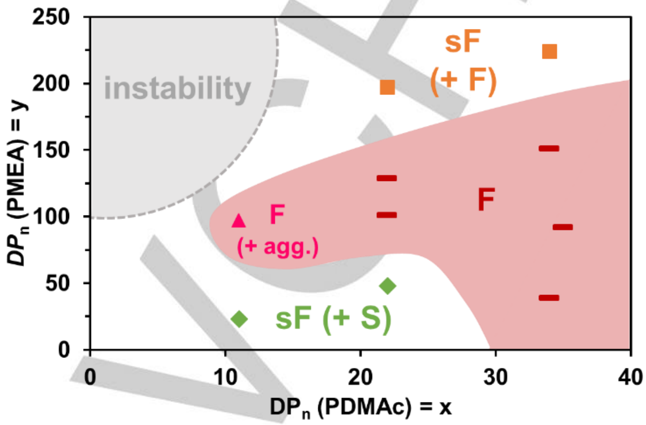

Figure 4. Pseudo phase diagram for **PDMAc$_x$-*b*-PMEA$_y$-TTC-U$_2$** diblock copolymers prepared at about 10 wt% of monomer. The red domain represents the pure long-fibre phase. Dash = fibres (F), square = mainly small fibres (sF) with few fibres, diamond = mainly small fibres with few spheres, triangle = fibres with few aggregates (agg.). Instability domain refers to colloidal stability issues.

To better understand the fibre formation mechanism, we monitored by cryo-TEM a typical dispersion polymerization (**U8**, Table S2, Figure S15). Initially, the macro-RAFT agent was apparently only partially organized into fibres (Figure S6B) - probably because of its limited hydrophobic domain.[36] However, at low monomer conversion, corresponding to a short hydrophobic block (*DP*$_n$ = 47), the amphiphilic polymer organized into long fibres. Contrary to conventional PISA, where the morphology changes with monomer conversion, the fibre morphology was maintained and a progressive increase of the diameter of the cylinders was observed from 16 nm (*DP*$_n$ = 47) to 28 nm (*DP*$_n$ = 224) (Figure S15). As mentioned above, beyond a certain degree of polymerization, the cylinder length seemed to decrease, probably because of the increasing steric hindrance of the growing hydrophobic block that outplays hydrogen-bonding driven interactions of the stickers in the core of the assemblies.[39,40]

These results show that the overwhelming formation of anisotropic structures in a large range of experimental conditions must be attributed to the directional assembly of the bis-urea stickers present in the macroRAFT agents. Even though the macroRAFT agents are initially not completely preorganized in fibre-like micelles, the formation of long fibres is observed once a sufficient number of hydrophobic monomer units is added, apparently stabilizing the assembly, and yielding long fibres through a templating mechanism. During the polymerization, the hydrogen-bonding driven assembly in the fibre core is maintained and the diameter of the fibres increases with increasing molar mass of the hydrophobic block as proposed in Scheme 2.

Scheme 2. Proposed mechanism of urea-templated PISA.

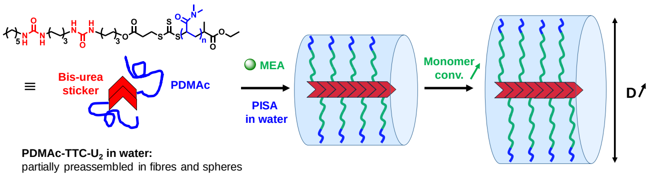

In order to assess that the proposed strategy is not limited to the described polymers, we have also tested a bis-urea-functional poly(acrylic acid) macroRAFT agent, PAA_{17}-TTC-U_2, in the proposed templated-PISA strategy (Table S5). Our first results show that the polymerization of MEA in the presence of PAA_{17}-TTC-U_2 leads to well-controlled copolymers self-assembled into long fibers (Figure S16), which makes us confident about the versatility of the system.

In summary, the introduction of a bis-urea sticker allows steering PISA towards anisotropic morphologies, while maintaining a good polymerization control. Reference experiments, and also former reports with MEA monomer in aqueous PISA, led to spheres only[42] or worms in very restricted conditions[43], whereas our templating strategy makes the synthesis of fibres very robust towards polymerization conditions, namely monomer and macroRAFT agent concentrations. Furthermore, while in conventional PISA the morphology relates to the molar mass of the blocks, and consequently the diameter of worms/fibres is not tunable but determined by the system, here, the diameter of the fibres can be tuned on demand *via* the M_n of the hydrophobic block. Currently, we further investigate the versatility of the system towards other monomers in order to produce nanofibres for various fields of application.

Acknowledgements

J.R. thanks the French Agence Nationale de la Recherche (PISAForFilms project, ANR-17-CE09-0031-01). The authors thank Patricia Beaunier for TEM measurements and Justine Elgoyhen for technical support.

Conflict of interest

The authors declare no conflict of interest.

Keywords: block copolymers • hydrogen bonds • nanofibers • self-assembly • supramolecular chemistry •

[1] B. Charleux, G. Delaittre, R. Rieger, F. D'Agosto, F., *Macromolecules* **2012**, *45*, 6753.

[2] N. J. Warren, S. P. Armes, *J. Am. Chem. Soc.* **2014**, *136*, 10174.

[3] S. L.Canning, G. N.Smith, S. P. Armes, *Macromolecules* **2016**, *49*, 1985.

[4] U. Tritschler, S. Pearce, J. Gwyther, G. R. Whittell, I. Manners, *Macromolecules* **2017**, *50*, 3439.

[5] M Lansalot, J. Rieger, F. D'Agosto, in *Macromolecular Self-assembly*, John Wiley & Sons, Inc., **2016**, pp. 33-82.

[6] J. Chiefari, Y. K. Chong, F. Ercole, J. Krstina, J. Jeffery, T. P. T. Le, R. T. A. Mayadunne, G. F. Meijs, C. L. Moad, G. Moad, E. Rizzardo, S. H. Thang, *Macromolecules* **1998**, *31*, 5559.

[7] J. N. Israelachvili, D. J.Mitchell, B. W. Ninham, *J. Chem. Soc. Faraday* Trans. 2 **1976**, *72*, 1525.

[8] A. Blanazs, S. P. Armes, A. J. Ryan, *Macromol. Rapid Commun.* **2009**, *30*, 267.

[9] J. Rieger, *Macromol. Rapid Commun.* **2015**, *36*, 1458.

[10] W. Zhang, F. D'Agosto, O. Boyron, J. Rieger, B. Charleux, *Macromolecules* **2012**, *45*, 4075.

[11] A. Blanazs, J. Madsen, G. Battaglia, A. J. Ryan, S. P. Armes, *J. Am. Chem. Soc.* **2011**, 133, 16581.

[12] A. Blanazs, R. Verber, O. O. Mykhaylyk, A. J. Ryan, J. Z. Heath, C. W. I. Douglas, S. P. Armes, *J. Am. Chem. Soc.* **2012**, *134*, 9741.

[13] W. Zhang, B. Charleux, P. Cassagnau, *Soft Matter* **2013**, *9*, 2197.

[14] W. Zhang, B. Charleux, P. Cassagnau, *Macromolecules* **2012**, *45*, 5273.

[15] R. Verber, A. Blanazs, S. P. Armes, *Soft Matter* **2012**, *8*, 9915.

[16] C. J. Mable, K. L. Thompson, M. J. Derry, O. O. Mykhaylyk, B. P. Binks, S. P. Armes, *Macromolecules* **2016**, *49*, 7897.

[17] R. Albigès, P. Klein, S. Roi, F. Stoffelbach, C. Creton, L. Bouteiller, J. Rieger, *Polym. Chem.* **2017**, *8*, 4992.

[18] A. Blanazs, A. J. Ryan, S. P. Armes, *Macromolecules* **2012**, *45*, 5099.

[19] S. J. Byard, M. Williams, B. E. McKenzie, A. Blanazs, S. P. Armes, *Macromolecules* **2017**, *50*, 1482.

[20] G. Mellot, P. Beaunier, J.-M.Guigner, L. Bouteiller, J. Rieger, F. Stoffelbach, *Macromol. Rapid Commun.* **2018**, DOI : 10.1002/marc.201800315.

[21] X. Wang, Z. An, *Macromol. Rapid Commun.* **2018**, DOI : 10.1002/marc.201800325.

[22] J. Tan, H. Sun, M. Yu, B. S. Sumerlin, L. Zhang, *ACS Macro Lett.*, **2015**, 4 (11), 1249–1253

[23] J. Yeow, J. Xu, C. Boyer, *ACS Macro Lett.*, **2015**, 4 (9), 984–990

[24] J. Yeow, O. R. Sugita, C. Boyer, *ACS Macro Lett.*, **2016**, *5* (5), 558–564

[25] Y. Mai, A. Eisenberg, *Chem. Soc. Rev.* **2012**, *41*, 5969.

[26] X. Wang, G. Guerin, H. Wang, Y. Wang, I. Manners, M. A. Winnik, *Science* **2007**, *317*, 644.

[27] L. Cao, I. Manners, M. A. Winnik, *Macromolecules* **2002**, *35*, 8258.

[28] D. Tao, C. Feng, Y. Lu, Y. Cui, X. Yang, I. Manners, M. A. Winnik, X. Huang, *Macromolecules* **2018**, *51*, 2065.

[29] N. Petzetakis, A. P. Dove, R. K. O'Reilly, *Chem. Sci.* **2011**, *2*, 955.

[30] E. Krieg, M. M. C. Bastings,P. Besenius, B. Rybtchinski, *Chem. Rev*. **2016**, *116*, 2414.

[31] S. H. Kim, F. Nederberg, R. Jakobs, J. P. K. Tan, K. Fukushima, A. Nelson, E. W. Meijer, Y. Y. Yang, J. L. Hedrick, *Angew. Chem. Int. Ed.* **2009**, *48*, 4508.

[32] J. D. Hartgerink, E. Beniash, S. I. Stupp, *PNAS* **2002**, *99*(8), 5133.

[33] S. C. Larnaudie, J. C. Brendel, K. A. Jolliffe, S. Perrier, *ACS Macro Lett.* **2017**, *6*, 1347.

[34] S.Han, E. Nicol, F. Niepceron, O. Colombani, S. Pensec, L. Bouteiller, *Macromol. Rapid. Commun.* **2018**, DOI : 10.1002/marc.201800698.

[35] N. Chebotareva, P. H. H. Bomans, P. M. Frederik, N. A. J. M. Sommerdijk, R. P. Sijbesma, *Chem. Commun*. **2005**, *0*, 4967.

[36] E. Obert, M. Bellot,L. Bouteiller, F. Andrioletti, C. Lehen-Ferrenbach, F. Boué, *J. Am. Chem. Soc.* **2007**, *129*, 15601.

[37] A. Pal, S. Karthikeyan, R. P. Sijbesma, *J. Am. Chem. Soc.* **2010***, 132*, 7842.

[38] M. Tharcis, T. Breiner, J. Belleney, F. Boué, L. Bouteiller, *Polym. Chem.* **2012**, *3*, 3093.

[39] S. Catrouillet, C. Fonteneau, L. Bouteiller, N. Delorme, E. Nicol, T. Nicolai, S. Pensec, O. Colombani, *Macromolecules* **2013**, *46*, 7911.

[40] X. Callies, C. Fonteneau, C. Vechambre, S. Pensec, J.-M. Chenal, L. Chazeau, L. Bouteiller, G. Ducouret, C. Creton, *Polymer* **2015**, *69*, 233.

[41] J. Rieger, G. Osterwinter, C. Bui, F. Stoffelbach, B. Charleux, *Macromolecules* **2009**, *42*, 5518.

[42] G. Liu, Q. Qiu, W. Shen, Z. An, *Macromolecules* **2011**, *44*, 5237.

[43] S. Sugihara, A. H. Ma'Radzi, S. Ida, S. Irie, T. Kikukawa, Y. Maeda, *Polymer* **2015**, *76*, 17.

Table of Contents

COMMUNICATION

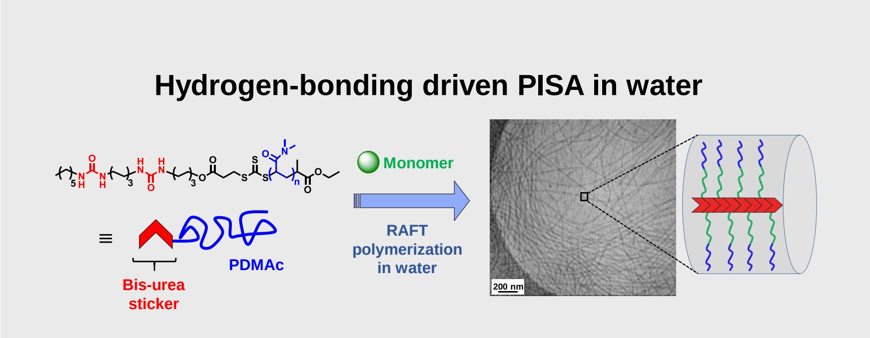

G. Mellot, J.-M. Guigner, L. Bouteiller, F. Stoffelbach*, and J. Rieger*

Page No. – Page No.

Templated-PISA: Driving Polymerization-Induced Self-Assembly towards the Fibre Morphology

Current limitations of polymerization-induced self-assembly (PISA) are overcome by combining RAFT polymerization and supramolecular chemistry: The introduction of supramolecular stickers into PISA allows the robust synthesis of long nanofibres with tunable diameter.